

First Principle Electronic Model for High-Temperature Superconductivity

V.I. Anisimov, M.A. Korotin, I.A. Nekrasov, and Z.V. Pchelkina
Institute of Metal Physics, Ekaterinburg GSP-170, Russia

S. Sorella
Istituto Nazionale per la Fisica della Materia, and SISSA, I-34014 Trieste, Italy
(Dated: 06 March 2002)

Using the structural data of the La_2CuO_4 compound both in the LTT phase and in the isotropic phase we have derived an effective $t - J$ model with hoppings t and superexchange interactions J extended up to fourth and second nearest neighbors respectively. By numerically studying this hamiltonian we have then reproduced the main experimental features of this HTc compound: d-wave superconductivity is stabilized at small but finite doping $\delta > 6\%$ away from the antiferromagnetic region and some evidence of dynamical stripes is found at commensurate filling $1/8$.

PACS numbers: 74.20.Mn, 71.10.Fd, 71.10.Pm, 71.27.+a

The microscopic mechanism of high-temperature superconductivity (HTc) is probably the most important, but still open problem in condensed matter physics. After the recent discovery of MgB_2 [1] – a phonon like superconductor with $T_c \simeq 39K$, and the fullerene superconductivity temperature [2] has been substantially enhanced in a compound where certainly the electron-phonon coupling cannot be neglected, there have been increasing expectations [3] that the conventional type of electron-phonon BCS superconductivity may explain all HTc materials [3]. On the other hand, from the theoretical point of view, a wide range of numerical techniques have recently led [4] to rather consistent evidence that strongly correlated models, such as Hubbard like [5], and $t - J$ models [6, 7] may show d-wave superconductivity at low temperature, evidence that is rather remarkable because no electron-phonon or explicit attractions are included in these models.

In order to contribute to the solution of these controversial aspects between theories and experiments and to understand the role of the strong electron correlation, in the present work we try to reduce the distance between the physics of rather abstract model hamiltonians and a consistent *ab-initio* derivation of experimental properties of HTc material. We consider the most popular compound for HTc superconductivity – La_2CuO_4 . We derive, and then study by Quantum Monte Carlo methods, an effective model in which the electron-phonon interaction is neglected. Our purpose is to understand whether the physics of an effective model hamiltonian may explain properties of real materials that are not understood with conventional methods of band theory and/or BCS mechanism of superconductivity. To our knowledge our work represents the first attempt to explain the physics of HTc superconductors, starting from first principle calculations.

The La_2CuO_4 compound is known to be superconductor in a range of doping between 6% and 30%, and by interstitial substitution of Nd (in place of La) at

commensurate filling $1/8$, static incommensurate peaks in the magnetic structure factor were observed by neutron scattering experiments [8] and, correspondingly, the superconducting transition temperature was strongly suppressed. The Nd-substitution enhances the spatial anisotropy and is believed to favor the formation of stripes: one dimensional hole-rich patterns in the CuO planes, separating antiferromagnetic (AF) domains with opposite direction of the AF order parameter, namely the next nearest neighbor Cu-spins across the stripe are antiparallel. This feature easily explains the mentioned neutron scattering incommensurate peaks, within the assumption that the stripes are half filled (half an hole per Cu site density along the stripe). In fact this implies that, at a given hole doping δ , the incommensurate peak in the magnetic structure factor $S(q)$ shifts by $2\pi\delta$ from the AF wavevector $(\pi, \pi) \rightarrow (\pi, \pi - 2\pi\delta)$ (for equally spaced stripes parallel to the x-axis direction), correspondingly the charge structure factor $N(q)$ shows up an incommensurate peak close to the Γ point for $q = (0, 4\pi\delta)$ [8].

We consider the extended $t - J$ one-band model on a finite lattice with N sites:

$$\mathcal{H} = \sum_{R,\mu} J_\mu \mathbf{S}_R \cdot \mathbf{S}_{R+\tau_\mu} - \sum_{R,\mu,\sigma} t_\mu \left(\tilde{c}_{R,\sigma}^\dagger \tilde{c}_{R+\tau_\mu,\sigma} + H.c. \right)$$

where $\tilde{c}_{i,\sigma}^\dagger = c_{i,\sigma}^\dagger (1 - n_{i,\bar{\sigma}})$, and \mathbf{S}_i is the electron spin operator on site i , whereas the sum run over the lattice sites R and corresponding neighbors $R + \tau_\mu$, determined by vectors τ_μ shown in Table I. Previous work have shown the key relevance of hoppings extended beyond nearest neighbors to reproduce the phenomenology of the Cuprates [9]. In this table we microscopically derive the values of the effective parameters t_μ and J_μ determined from the results of electronic structure calculations by standard LDA (TBLMTO [10]) and LDA+U method [11], for the anisotropic case (with Nd substitution) and the high-symmetry tetragonal case, using known structural data [12]. The effective hopping parameters t_μ were calculated by the standard least-square fit

TABLE I: Values of the effective parameters in eV.

τ	Anisotropic		Isotropic	
	J_μ	t_μ	J_μ	t_μ
(1,0)	0.105	0.425	0.109	0.486
(0,1)	0.111	0.466	0.109	0.486
(1,1)	0.016	0.014	0.016	-0.086
(2,0)	0	0.036	0	-0.006
(0,2)	0	-0.064	0	-0.006
(2,1)	0	-0.001	0	0
(1,2)	0	0.046	0	0

procedure to the bands obtained in LMTO calculations. The effective exchange parameters J_μ were calculated using the formula derived by A. Lichtenstein [13, 14], where the second derivative of the total energy as a function of the value of the angle between spin directions on two atoms is calculated via eigenvalues and eigenfunctions obtained in electronic structure calculations. Those electronic structure calculations were done using LDA+U method which allows to obtain antiferromagnetic insulating ground state for the undoped cuprate. By contrast, the standard LDA method leads to a nonmagnetic metallic ground state [11], which is obviously inconsistent with experiments. The Coulomb parameters U and J used in LDA+U calculations were obtained in constrained LDA calculation [15] ($U=11$ eV, $J=1$ eV).

The Nd-substitution for La in La_2CuO_4 results in anisotropic Low Temperature Tetragonal (LTT) structure [12] (Fig.1), where the CuO_6 tetrahedra are tilted via rotation around $[1,0]$ axis (and $[0,1]$ axis in the next plane, so that the total crystal structure preserves tetragonal symmetry). As a result of this tilting there are two kinds of oxygen atoms, O1 which form 180 degree Cu-O-Cu bonds in $[1,0]$ direction and are in the Cu atoms plane, and O2 atoms, which are shifted out of the plane and form Cu-O-Cu bonds in $[0,1]$ direction with the decreased bond angle. Remarkably the strongest nearest neighbor hopping is in the direction $[0,1]$ where the oxygen atoms are out of the Cu-Cu plane (see Fig. 1). This seems counterintuitive, because for this direction the Cu-O-Cu bond angle is less than 180 degree and hence the effective d-d hopping must be decreased comparing with the straight Cu-O-Cu bond in $[1,0]$ direction. Solution of this puzzle is the difference in electrostatic potential on O1 and O2 crystallographic positions which results in the energy of 2p-orbitals of out-of-plane O2 atoms being 1.05 eV higher than for the in-plane O1 atom. As the effective d-d hopping is proportional to t_{pd}^2/Δ_{pd} , where t_{pd} is effective p-d hopping parameter and Δ_{pd} is energy separation between Cu-3d and O-2p orbitals, then Δ_{pd} is significantly smaller for out-of-plane O2 oxygen resulting in a larger value of the effective d-d hopping parameter. Another effect of anisotropic crystal structure distortion

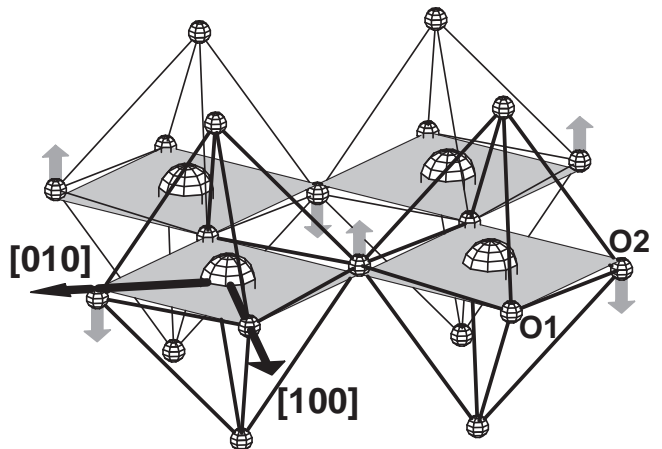


FIG. 1: Structural data for the HTc materials considered (see text). The displacements of the ions in the anisotropic LTT phase is indicated by the arrows.

is the long-range nature of model hamiltonian hopping parameters. For the isotropic case only two shells of nearest neighbors were needed and the value of t_μ for the third neighbor is negligible. Instead for the anisotropic case the hopping parameters have to extend at least up to fourth neighbors for a satisfactory fit of the LMTO bands. We must note also, that the usual scaling of the effective exchange parameters J_μ as t_μ^2 is not valid here.

In order to study this model hamiltonian we use the recent QMC methods, that have been shown to work very well for the standard $t - J$ model [16], allowing to obtain very accurate values of energies and correlation functions for a wide range of J/t values. The initial variational wavefunction is chosen to be the most general Jastrow-BCS real wavefunction $\psi_G = \hat{J}|BCS\rangle$ projected onto the subspace with no-doubly occupied sites and fixed number of particles. After the latter projection the wavefunction is totally symmetric, and a large number of variational parameters can be optimized consistently with the symmetries of the model. This is the first step $p = 0$ of our procedure (SR) [16, 17] (e.g. 46 variational parameters for the 8×8 anisotropic case), which is in principle convergent for large number p of iterations. The scheme is based on the fast convergence properties of the Lanczos technique, that allows to improve remarkably the accuracy of the best variational guess with few iterations. Starting from the p -Lanczos step wavefunction it is also possible to further improve the variational energy and especially the quality of the correlation functions, by a further correction scheme, such as the fixed node (FN) [18] or the more accurate stochastic reconfiguration method (SR) [17]. A comparison of the quality of our approximation, as compared with the conventional Fixed node technique [18] is shown in Tab. II.

We concentrate our study in the low-doping region and especially at the important filling $\delta = 1/8$ where

TABLE II: Variational energy (eV) per Cu site for the anisotropic $t - J$ (Tab. I) model for the best variational FN and SR ($p = 2$) techniques applied to the $p = 1$ Lanczos wavefunction. The $\sigma = 0$ are estimates of the exact zero variance energies [16]. Error bars are in brackets.

# Holes	VMC	FN	SR	$\sigma = 0$
0	-0.06446(1)	-0.06614(4)	-0.06637(4)	-0.06665(17)
4	-0.12717(3)	-0.1368(1)	-0.1379(1)	-0.1402(5)
6	-0.15623(4)	-0.1679(1)	-0.1701(2)	-0.1744(14)
8	-0.18336(4)	-0.1972(1)	-0.1988(3)	-0.2025(7)
10	-0.20859(4)	-0.2237(1)	-0.2265(3)	-0.2316(6)
16	-0.27446(6)	-0.2929(1)	-0.2956(4)	-0.3053(11)
26	-0.35030(6)	-0.3684(1)	-0.3710(4)	-0.3780(12)

static stripes were observed. As shown in Fig. 2 there is a clear evidence, especially in the anisotropic case, of an incommensurate peak that was not present at the variational level, and is sharpening as the accuracy of the calculation approaches the low energy limit. Correspondingly the charge structure factor $N(q)$ does not seem to be enhanced in this limit, but only a cusp singularity at the Tranquada's wavevector appears consistent with our data. The strongest anisotropy appears in the nearest neighbor hoppings (see Tab. 1) and, correspondingly the peak in the magnetic structure factor, is shifted by $(0, 2\pi\delta)$, consistent with the Tranquada's predictions. Within the "stripe picture" this is compatible with stripes along the $[1, 0]$ axis, a direction where the nearest neighbor hopping is much less favored compared with the other direction. Thus, in order to optimize the kinetic energy in the y -direction, charge-fluctuations perpendicular to the stripes are required. These fluctuations suppress any static response in the charge structure factor, but leave a sizable effect in the spin provided the spins across the hole are antiparallel [19], as we have verified in this case. In the following we name this feature the "dynamical stripe", a genuine effect of strong correlation.

As shown in Fig. 2, the anisotropy clearly enhances the dynamical stripe fluctuations, since, in the anisotropic case, a more resolved incommensurate peak for $S(q)$ is found. Some small effect is seen also in the isotropic case, consistent with the DMRG findings [7] that $t'/t < 0$ may stabilize stripes. Probably at very low energy (larger p) evidence of true static stripes can also be found at this particular filling. For all other dopings, though incommensurate magnetic peaks are still present, they are much less sharp, and the value of $S(q)$ at the maximum is much below the corresponding $p = 0$ variational value.

Regarding superconductivity, we have studied the pairing correlation functions $\Delta_i^{\mu,\nu}(r) = \langle \mathcal{S}_{i+r,\mu} \mathcal{S}_{i,\nu}^\dagger \rangle$. Here $\mathcal{S}_{i,\mu}^\dagger = \tilde{c}_{i,\uparrow}^\dagger \tilde{c}_{i+\mu,\downarrow}^\dagger - \tilde{c}_{i,\downarrow}^\dagger \tilde{c}_{i+\mu,\uparrow}^\dagger$ creates an electron singlet pair in the neighboring sites $(i, i + \mu)$. Off-diagonal long-range order is implied if $P_d = 2 \lim_{r \rightarrow \infty} \sqrt{|\Delta_i^{\mu,\nu}(r)|}$ remains fi-

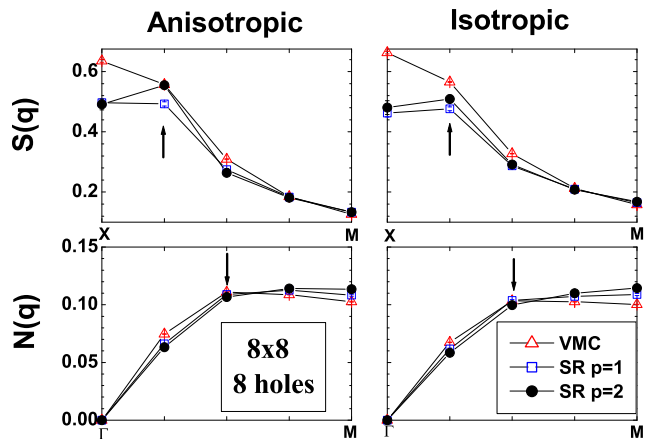


FIG. 2: Spin and charge structure factors for the cases of Tab. I vs. improved accuracy in energy: VMC, SR $p=1$, SR $p=2$, respectively. $\Gamma = (0, 0)$. $X = (\pi, \pi)$, $M = (\pi, 0)$, $\underline{M} = (0, \pi)$ and the arrows indicate the Tranquada's wavevectors (see text).

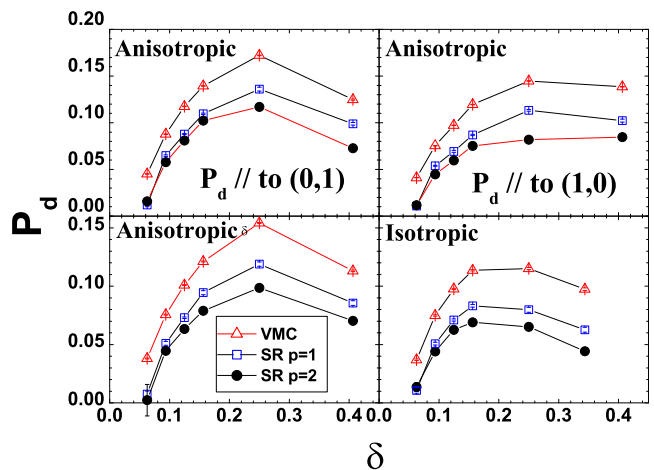


FIG. 3: P_d for various dopings and improved accuracy in energy, VMC, SR $p=1$, and SR $p=2$, respectively, for the cases of Tab. I. Lower panels: the value of P_d was obtained by d -wave-averaging the pairing correlations at the maximum distance $\simeq 4\sqrt{2}$. Upper ones: P_d refers to the maximum distance ($= 4$) along the x, y directions.

nite in the thermodynamic limit.

For the 8×8 system, that we have studied for several dopings (see Fig. 3 lower panels) size effects are acceptable, at least close to optimal doping as shown in [6] for the $t - J$ model. The existence of a finite P_d and correspondingly the absence of antiferromagnetic long range order is an experimental fact for $\delta > 6\%$. Both features are remarkably well reproduced by our calculations (see right Fig. 4). In particular, at half filling, the magnetic structure factor dramatically increases with respect to the spin liquid variational wavefunction $\hat{J}|BCS\rangle$, confirming the existence of AF long range order, as widely accepted for the weakly frustrated Heisenberg model.

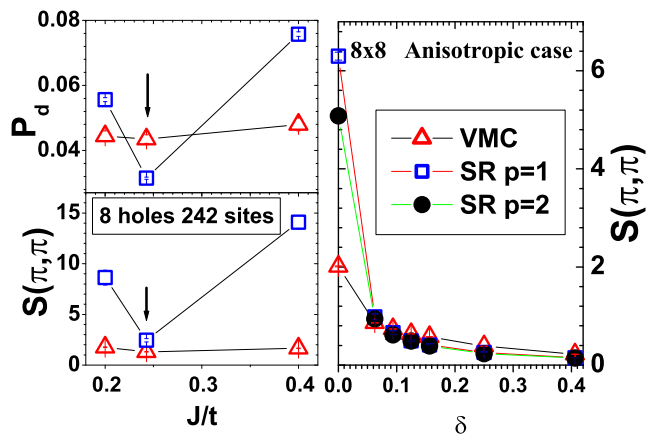


FIG. 4: Right panel: $S(\pi, \pi)$, as a function of doping δ for the 8×8 anisotropic (Tab. I) $t-J$ model. Left panels: $S(\pi, \pi)$ and P_d for larger size for the standard $t-J$ model (including the nearest neighbor density-density interaction, which however is irrelevant at small doping) and the anisotropic case indicated by the arrow. In the latter case the J/t value is defined by the average nearest neighbor ratio.

Conversely, as soon as the doping is thinly increased, the AF magnetic structure factor remains very close to the spin liquid variational reference, clearly indicating absence of AF long range order. This is the main result of our paper and is due to the long range couplings of our effective model, since at small doping the $t-J$ model without long range couplings is expected to be both antiferromagnetic and superconductor [6]. In order to understand this effect, we have extended the calculation to larger size $N = 242$ at small doping both for the standard $t-J$ model at $J/t = 0.2$ and $J/t = 0.4$ and our extended $t-J$ model, in the anisotropic case. As it is clearly seen in the left panels of Fig. 4, the role of the long range hoppings is crucial to destroy both antiferromagnetism and superconductivity.

Another effect is that, within our model, the anisotropy does not suppress the superconducting order parameter P_d , (see lower Fig. 3). This is rather in contrast with experiments, where a drastic change of T_c was found in the anisotropic case. However in this case the pairing correlations are also anisotropic (see upper Fig.3) and P_d vs doping, computed at the maximum $[1, 0]$ or $[0, 1]$ distance appears to be much suppressed in the direction of the stripe (notice that this direction is alternatively x or y in neighboring CuO planes). It is possible that by including the electron-phonon coupling one can obtain further agreement with experiments. In fact we expect that, whenever dynamical stripes are clearly formed, the electron-phonon coupling can considerably enhance the anisotropy and lead to the formation of true static stripes, with negligible P_d .

In conclusion we can reproduce many aspects of the low-doping phase diagram of HTc compounds by neglect-

ing completely the electron phonon coupling, within an *ab-initio* derivation of the effective superexchange and long-range hopping couplings for an extended $t-J$ model. Several interesting features comes out from our calculation that deserve experimental confirmation: the finite critical doping δ_c required to stabilize superconductivity, appears a band structure effect. In principle antiferromagnetism and superconductivity may coexist at small enough doping, provided the long range hoppings are suppressed. The anisotropy and long range hoppings appear to be compatible with a sizable superconducting order parameter, as long as the stripes remain dynamical [20]. Static stripes are not clearly stabilized in a model in which the electron-phonon interaction is disregarded.

This work was partially supported by Russian foundation for Basic Research grant RFFI-01-02-17063 and by MIUR-COFIN2001. We acknowledge T.M. Rice for stimulating the present scientific collaboration and E. Dagotto for useful discussions.

-
- [1] J. Nagamatsu *et al.*, Nature (London), **410**, 63 (2001).
 - [2] J.H. Schoï, Ch. Kloc, B. Batlogg, Science, **293**, 2432 (2001).
 - [3] A. Lanzara *et al.* Nature **412**, 510 (2001).
 - [4] see e.g. P.W. Anderson cond-mat/0201429 (2002).
 - [5] Th. Maier *et al.* Phys. Rev. Lett. **86**, 129 (2001).
 - [6] S. Sorella *et al.* cond-mat/0110460, to be published in Phys. Rev. Letters.
 - [7] S.R. White and D. Scalapino, Phys. Rev. Lett. **80** 1272 (1998); *ibidem* Phys. Rev. B **60**, 753 (1999).
 - [8] J.M. Tranquada *et al.*, Nature **375**, 561 (1995), J.M. Tranquada *et al.*, Phys. Rev. Lett. **78**, 338 (1997).
 - [9] A. Nazarenko *et al.* Phys. Rev. B **51**, 8676 (1995); P.W. Leung *et al.* Phys. Rev. B **56**, 630 (1997).
 - [10] O.K. Andersen, and O. Jepsen, Phys. Rev. Lett **53**, 2571 (1984). O.K. Andersen, Z. Pawlowska, and O. Jepsen, Phys. Rev. B **34**, 5253 (1986)
 - [11] V.I. Anisimov, J. Zaanen and O.K. Andersen, Phys. Rev. B **44**, 943 (1991); V.I. Anisimov, F. Aryasetiawan, A.I. Lichtenstein, J. Phys.: Condens. Matter **9**, 767 (1997).
 - [12] Journal of Low Temperature Physics, **95**, 271 (1994).
 - [13] A.I. Lichtenstein, M.I. Katsnelson, V.P. Antropov, V.A. Gubanov, J. Magn. Magn. Mater. **67**, 65 (1987).
 - [14] A.I. Liechtenstein V.I. Anisimov and J. Zaanen Phys. Rev. B **52** R5467 (1995)
 - [15] O. Gunnarsson, O.K. Andersen, O. Jepsen, J. Zaanen, Phys. Rev. B **39**, 1708 (1989); V.I. Anisimov and O. Gunnarsson, Phys. Rev. B **43**, 7570 (1991).
 - [16] S. Sorella Phys. Rev. B **64** 024512 (2001).
 - [17] S. Sorella cond-mat/0201388, lecture notes for the Euro-Winter School Kerkade-NL (2002).
 - [18] D.F.B. ten Haaf, J.M.J. van Leeuwen, W. van Saarloos, and D.M. Ceperley, Phys. Rev. B **51**, 13039 (1995).
 - [19] G.B. Martins *et al.*, Phys. Rev. Lett. **84**, 5844 (2000).
 - [20] E. Pavarini *et al.* Phys. Rev. Lett. **87** 047003 (2001).